Published by Institute of Physics Publishing for SISSA/ISAS
Received: *November 22, 2001*
Accepted: *December 6, 2001*

Direct Higgs production and jet veto at the Tevatron and the LHC in NNLO QCD*

Stefano Catani†
Theory Division, CERN, CH-1211 Geneva 23, Switzerland
E-mail: Stefano.Catani@cern.ch

Daniel de Florian‡
Departamento de Física, FCEYN, Universidad de Buenos Aires
(1428) Pabellón 1 Ciudad Universitaria, Capital Federal, Argentina
E-mail: deflo@df.uba.ar

Massimiliano Grazzini
Dipartimento di Fisica, Università di Firenze
I-50019 Sesto Fiorentino, Florence, Italy
INFN, Sezione di Firenze
I-50019 Sesto Fiorentino, Florence, Italy
E-mail: grazzini@fi.infn.it

Abstract: We consider Higgs boson production through gluon-gluon fusion in hadron collisions, when a veto is applied on the transverse momenta of the accompanying hard jets. We compute the QCD radiative corrections to this process at NLO and NNLO. The NLO calculation is complete. The NNLO calculation uses the recently evaluated NNLO soft and virtual QCD contributions to the inclusive cross section. We find that the jet veto reduces the impact of the NLO and NNLO contributions, the reduction being more sizeable at the LHC than at the Tevatron.

Keywords: Higgs Physics, QCD, Hadronic Colliders.

*This work was supported in part by the EU Fourth Framework Programme "Training and Mobility of Researchers", Network "Quantum Chromodynamics and the Deep Structure of Elementary Particles", contract FMRX–CT98–0194 (DG 12 – MIHT).

†On leave of absence from INFN, Sezione di Firenze, Florence, Italy.

‡Partially supported by CONICET and Fundación Antorchas.

JHEP01(2002)015

Contents

JHEP01(2002)015

1. Introduction

The mechanism of electroweak symmetry breaking is one of the main issues in high-energy particle physics. In the Standard Model (SM) and in its supersymmetric extensions the mechanism is accomplished by elementary scalar doublets. The Higgs boson(s) [1] are thus a fundamental ingredient of the theory, and their search is the main goal of current and future colliders.

The direct search at LEP implies a lower limit of $M_H > 114.1\,\text{GeV}$ (at 95% CL) [2] on the mass M_H of the SM Higgs boson, and shows an excess of events, which may indicate the production of a Higgs boson with mass near 115 GeV [3, 4, 2]. Global SM fits to electroweak precision measurements favour a light Higgs ($M_H \lesssim 200\,\text{GeV}$) [5].

After the end of the LEP era, the search for the Higgs boson will be carried out at hadron colliders. Depending on the luminosity delivered to the CDF and D0 detectors during the forthcoming Run II, the Tevatron experiments can yield evidence for a Higgs boson with $M_H \lesssim 180\,\text{GeV}$ and may be able to discover (at the 5σ level) a Higgs boson with $M_H \lesssim 130\,\text{GeV}$ [6]. At the LHC, the SM Higgs boson can be discovered over the full mass range up to $M_H \sim 1\,\text{TeV}$ after a few years of running [7].

The dominant mechanism for SM Higgs boson production at hadron colliders is gluon-gluon fusion through a heavy-quark (top-quark) loop [8]. This mechanism is often called *direct* Higgs production, to distinguish it from *associated* production of Higgs boson and vector bosons, heavy quarks, jets, and so forth. The next-to-dominant mechanism [6, 7] for the production of SM Higgs bosons at the Tevatron and the LHC is weak boson fusion.

At the LHC [9], gg fusion exceeds all the other production channels by a factor decreasing from 8 to 5 when M_H increases from 100 to 200 GeV. When M_H approaches 1 TeV, gg fusion still provides about 50% of the total production cross section. At low values of M_H the dominant decay mode is $H \to b\bar{b}$, but it is swamped by the QCD background. This decay mode is thus exploited [7] in the low-mass range $100\,\text{GeV} \lesssim M_H \lesssim 120\,\text{GeV}$ only

in the case of the associated production $Ht\bar{t}$. In the case of direct production, the most important decay channels for Higgs searches [7] are the rare decay $H \to \gamma\gamma$ in the low-mass range $100\,\mathrm{GeV} \lesssim M_H \lesssim 140\,\mathrm{GeV}$, and the channel $H \to ZZ \to 4l$ in the mass range $130\,\mathrm{GeV} \lesssim M_H \lesssim 700\,\mathrm{GeV}$. In the intermediate-mass region $150\,\mathrm{GeV} \lesssim M_H \lesssim 190\,\mathrm{GeV}$, direct Higgs production followed by the decay $H \to WW \to l^+l^-\nu\bar{\nu}$ is also relevant. The strong angular correlations of the final-state leptons from W decay are an important ingredient for this discovery channel [10].

At the Tevatron, gg fusion remains the main production channel [6], but it is experimentally less important than at the LHC because the decay rate $H \to \gamma\gamma$ is too low to be observed. When $M_H \lesssim 135\,\mathrm{GeV}$, the most promising discovery mechanism [6] is thus the associated production ($q\bar{q} \to V^* \to HV$) of the Higgs boson with a vector boson V ($V = W$ or Z), whose leptonic decay provides the trigger for the signal from $H \to b\bar{b}$. Nevertheless, since the decays $H \to W^*W^*, Z^*Z^*$ have increasing branching fractions for $M_H \gtrsim 130\,\mathrm{GeV}$, $gg \to H \to W^*W^*, Z^*Z^*$ are the natural channels to consider when $140\,\mathrm{GeV} \lesssim M_H \lesssim 180\,\mathrm{GeV}$. In particular, the decay mode $W^*W^* \to l^+l^-\nu\bar{\nu}$ is quite important [11, 6], since it is cleaner than $W^*W^* \to l\nu jj$, and the decay rate $H \to W^*W^*$ is higher than $H \to Z^*Z^*$ by about one order of magnitude.

An important background for the direct Higgs signal $H \to W^*W^* \to l^+l^-\nu\bar{\nu}$ is $t\bar{t}$ production (tW production is also important at the LHC), where $t \to l\bar{\nu}b$, thus leading to b jets with high p_T in the final state. If the b quarks are not identified, a veto cut on the transverse momenta of the jets accompanying the final-state leptons can be applied to enhance the signal/background ratio. Imposing a jet veto turns out to be essential, both at the Tevatron [6, 11] and at the LHC [7], to cut the hard b jets arising from this background process.

The next-to-leading order (NLO) QCD corrections to gg fusion are large [12, 13, 14]. Approximate evaluations [15] of higher-order terms suggest that their effect can still be sizeable. The computation of the next-to-next-to-leading order (NNLO) corrections is thus important to better estimate the cross section for direct Higgs production.

Recently two groups [16, 17] have performed a first step in this direction, by evaluating the soft and virtual contributions to the NNLO partonic cross section $\hat{\sigma}(gg \to H+X)$ in the large-M_{top} approximation. Our calculation [16] was performed by combining Harlander's result [18] for the two-loop amplitude $gg \to H$ with the soft factorization formulae for tree-level [19, 20] ($gg \to Hgg, Hq\bar{q}$) and one-loop [21, 22] ($gg \to Hg$) amplitudes, and then using the technique of ref. [23]. The independent calculation of ref. [17] used a different method, and the analytical results fully agree.

In ref. [16] we also studied the quantitative impact of the soft and virtual NNLO contributions on direct Higgs boson production at the LHC. This was consistently done by using the recent MRST2000 set of parton distribution functions [24], which includes (approximated [25]) NNLO densities. In this paper we first perform an analogous study[1] at the Tevatron Run II, and we show that the soft and virtual contributions are expected to give a fairly good estimate of the complete NNLO result.

[1] Part of these results was anticipated in ref. [26].

In the second part of the paper we study the effect of a jet veto on direct Higgs production beyond the leading order (LO). We present new NLO and NNLO calculations for the vetoed cross section both at the Tevatron and at the LHC. These calculations are performed by subtracting the LO (NLO) cross section for the production of Higgs plus jets from the corresponding inclusive NLO (NNLO) cross section. The LO and NLO subtracted cross section for the production of Higgs plus jets is evaluated in the large-$M_{\rm top}$ limit, but without any soft and virtual approximations. At LO we derive analytical expressions, while at the NLO we use the numerical program of ref. [27].

The paper is organized as follows. In section 2 we recall the theoretical framework and the analytical results for the soft and virtual NNLO corrections. In section 3 we present the results for inclusive Higgs production at the Tevatron Run II. In section 4 we present the results obtained by applying a jet veto on the inclusive cross section, both at the Tevatron Run II and at the LHC. Our conclusions are summarized in section 5.

2. Inclusive QCD cross section at NNLO

We consider the collision of two hadrons h_1 and h_2 with centre-of-mass energy $\sqrt{s}$. The inclusive cross section for the production of the SM Higgs boson can be written as

$$\sigma(s,M_H^2) = \sum_{a,b} \int_0^1 dx_1\, dx_2\, f_{a/h_1}(x_1,\mu_F^2)\, f_{b/h_2}(x_2,\mu_F^2) \int_0^1 dz\, \delta\!\left(z - \frac{\tau_H}{x_1 x_2}\right) \times \\ \times\, \sigma_0\, z\, G_{ab}\left(z;\alpha_{\rm S}(\mu_R^2), \frac{M_H^2}{\mu_R^2}; \frac{M_H^2}{\mu_F^2}\right), \tag{2.1}$$

where $\tau_H = M_H^2/s$, and μ_F and μ_R are factorization and renormalization scales, respectively. The parton densities of the colliding hadrons are denoted by $f_{a/h}(x,\mu_F^2)$ and the subscript a labels the type of massless partons ($a = g, q_f, \bar{q}_f$, with N_f different flavours of light quarks). We use parton densities as defined in the $\overline{\rm MS}$ factorization scheme.

From eq. (2.1) the cross section $\hat{\sigma}_{ab}$ for the partonic subprocess $ab \to H + X$ at the centre-of-mass energy $\hat{s} = x_1 x_2 s = M_H^2/z$ is

$$\hat{\sigma}_{ab}(\hat{s},M_H^2) = \frac{1}{\hat{s}}\, \sigma_0 M_H^2\, G_{ab}(z) = \sigma_0\, z\;\; G_{ab}(z)\,, \tag{2.2}$$

where the term $1/\hat{s}$ corresponds to the flux factor and leads to an overall z factor. The Born-level cross section σ_0 and the hard coefficient function G_{ab} arise from the phase-space integral of the matrix elements squared.

Equation (2.1) can also be recast in the form

$$\sigma(s,M_H^2) = \sigma_0\, \tau_H \sum_{a,b} \int_{\tau_H}^1 \frac{d\tau}{\tau}\, \mathcal{L}_{ab/h_1h_2}(\tau,\mu_F^2)\, G_{ab}(\tau_H/\tau)\,, \tag{2.3}$$

where the function

$$\mathcal{L}_{ab/h_1h_2}(\tau,\mu_F^2) = \int_\tau^1 \frac{dx}{x} f_{a/h_1}(x,\mu_F^2) f_{b/h_2}(\tau/x,\mu_F^2) \tag{2.4}$$

is the parton luminosity that weights the event initiated by partons a and b.

The incoming partons a, b couple to the Higgs boson through heavy-quark loops and, therefore, σ_0 and G_{ab} also depend on the masses M_Q of the heavy quarks. The Born-level contribution σ_0 is [8]

$$\sigma_0 = \frac{G_F}{288\pi\sqrt{2}} \left| \sum_Q A_Q\left(\frac{4M_Q^2}{M_H^2}\right) \right|^2 , \tag{2.5}$$

where $G_F = 1.16639 \times 10^{-5}\,\mathrm{GeV}^{-2}$ is the Fermi constant, and the amplitude A_Q is given by

$$\begin{aligned} A_Q(x) &= \frac{3}{2} x \Big[1 + (1-x) f(x) \Big] , \\ f(x) &= \begin{cases} \arcsin^2 \dfrac{1}{\sqrt{x}} , & x \geq 1 \\ -\dfrac{1}{4} \left[\ln \dfrac{1+\sqrt{1-x}}{1-\sqrt{1-x}} - i\pi \right]^2 , & x < 1 . \end{cases} \end{aligned} \tag{2.6}$$

In the following we limit ourselves to considering the case of a single heavy quark, the top quark, and $N_f = 5$ light-quark flavours. We always use M_{top} ($M_{\mathrm{top}} = 176\,\mathrm{GeV}$) to denote the on-shell pole mass of the top quark.

The coefficient function G_{ab} in eq. (2.1) is computable in QCD perturbation theory according to the expansion

$$\begin{aligned} G_{ab}\left(z; \alpha_{\mathrm{S}}(\mu_R^2), \frac{M_H^2}{\mu_R^2}; \frac{M_H^2}{\mu_F^2}\right) &= \alpha_{\mathrm{S}}^2(\mu_R^2) \sum_{n=0}^{+\infty} \left(\frac{\alpha_{\mathrm{S}}(\mu_R^2)}{\pi}\right)^n G_{ab}^{(n)}\left(z; \frac{M_H^2}{\mu_R^2}; \frac{M_H^2}{\mu_F^2}\right) \\ &= \alpha_{\mathrm{S}}^2(\mu_R^2) G_{ab}^{(0)}(z) + \frac{\alpha_{\mathrm{S}}^3(\mu_R^2)}{\pi} G_{ab}^{(1)}\left(z; \frac{M_H^2}{\mu_R^2}; \frac{M_H^2}{\mu_F^2}\right) + \\ &\quad + \frac{\alpha_{\mathrm{S}}^4(\mu_R^2)}{\pi^2} G_{ab}^{(2)}\left(z; \frac{M_H^2}{\mu_R^2}; \frac{M_H^2}{\mu_F^2}\right) + \mathcal{O}(\alpha_{\mathrm{S}}^5) , \end{aligned} \tag{2.7}$$

where the (scale-independent) LO contribution is

$$G_{ab}^{(0)}(z) = \delta_{ag}\, \delta_{bg}\, \delta(1-z) . \tag{2.8}$$

Throughout the paper we work in the framework of the large-M_{top} expansion, where one can exploit the effective-lagrangian approach [28, 29, 15] to embody the heavy-quark loop in an effective vertex. However, unless otherwise stated, we include in σ_0 the full dependence on M_{top}. This approximation [14, 15] turns out to be very good when $M_H \leq 2M_{\mathrm{top}}$, and it is still accurate[2] to better than 10% when $M_H \lesssim 1\,\mathrm{TeV}$.

The NLO coefficients $G_{ab}^{(1)}(z)$ are known [12, 14]. Their explicit expressions (see e.g. ref. [16]) contain three kinds of contributions:

[2]The accuracy of this approximation when $M_H \lesssim 2M_{\mathrm{top}}$ may not be accidental. In fact, as discussed in the following, the main part of the QCD corrections to direct Higgs production is due to parton radiation at relatively low transverse momenta. Such radiation is weakly sensitive to the mass of the heavy quark in the loop.

JHEP01(2002)015

- Virtual and soft contributions, which are respectively proportional to $\delta(1-z)$ and to the distributions $\mathcal{D}_i(z)$, where

$$\mathcal{D}_i \equiv \left[\frac{\ln^i(1-z)}{1-z}\right]_+ . \tag{2.9}$$

  These are the most singular terms when $z \to 1$.

- Purely collinear logarithmic contributions of the type $\ln^i(1-z)$. These contributions give the next-to-dominant singular terms when $z \to 1$.

- Hard contributions, which are finite in the limit $z \to 1$.

The soft-virtual (SV) approximation is defined [16] by keeping only the terms proportional to $\delta(1-z)$ and $\mathcal{D}_i(z)$ in the coefficient G_{ab}. In this approximation only the gg channel contributes and we have

$$G_{ab}^{(1)\mathrm{SV}}(z; M_H^2/\mu_R^2; M_H^2/\mu_F^2) = \delta_{ag}\delta_{bg}\Bigg[\delta(1-z)\left(\frac{11}{2} + 6\zeta(2) + \frac{33-2N_f}{6}\ln\frac{\mu_R^2}{\mu_F^2}\right) + \\ + 6\mathcal{D}_0\,\ln\frac{M_H^2}{\mu_F^2} + 12\,\mathcal{D}_1\Bigg]. \tag{2.10}$$

The NNLO coefficients $G_{ab}^{(2)}$ are not yet completely known, but their SV approximation has been computed in refs. [16, 17]. It reads:

$$\begin{aligned} G_{gg}^{(2)\mathrm{SV}}\left(z; \frac{M_H^2}{\mu_R^2}, \frac{M_H^2}{\mu_F^2}\right) = \delta(1-z)\Bigg[&\frac{11399}{144} + \frac{133}{2}\zeta(2) - \frac{9}{20}\zeta(2)^2 - \frac{165}{4}\zeta(3) + \\ &+ \left(\frac{19}{8} + \frac{2}{3}N_f\right)\ln\frac{M_H^2}{M_{\mathrm{top}}^2} + \\ &+ N_f\left(-\frac{1189}{144} - \frac{5}{3}\zeta(2) + \frac{5}{6}\zeta(3)\right) + \\ &+ \frac{(33-2N_f)^2}{48}\ln^2\frac{\mu_F^2}{\mu_R^2} - 18\,\zeta(2)\ln^2\frac{M_H^2}{\mu_F^2} + \\ &+ \left(\frac{169}{4} + \frac{171}{2}\zeta(3) - \frac{19}{6}N_f + (33-2N_f)\zeta(2)\right)\ln\frac{M_H^2}{\mu_F^2} + \\ &+ \left(-\frac{465}{8} + \frac{13}{3}N_f - \frac{3}{2}(33-2N_f)\,\zeta(2)\right)\ln\frac{M_H^2}{\mu_R^2}\Bigg] + \\ +\mathcal{D}_0\Bigg[&-\frac{101}{3} + 33\zeta(2) + \frac{351}{2}\zeta(3) + N_f\left(\frac{14}{9} - 2\zeta(2)\right) + \\ &+ \left(\frac{165}{4} - \frac{5}{2}N_f\right)\ln^2\frac{M_H^2}{\mu_F^2} - \frac{3}{2}(33-2N_f)\ln\frac{M_H^2}{\mu_F^2}\,\ln\frac{M_H^2}{\mu_R^2} + \\ &+ \left(\frac{133}{2} - 45\zeta(2) - \frac{5}{3}N_f\right)\ln\frac{M_H^2}{\mu_F^2}\Bigg] + \end{aligned}$$

$$
\begin{aligned}
&+\mathcal{D}_1\Bigg[133-90\zeta(2)-\frac{10}{3}N_f+36\ln^2\frac{M_H^2}{\mu_F^2}+\\
&\qquad+(33-2N_f)\left(2\ln\frac{M_H^2}{\mu_F^2}-3\ln\frac{M_H^2}{\mu_R^2}\right)\Bigg]+\\
&+\mathcal{D}_2\left[-33+2N_f+108\ln\frac{M_H^2}{\mu_F^2}\right]\\
&+72\,\mathcal{D}_3\,. \qquad (2.11)
\end{aligned}
$$

To give a rough idea of the numerical hierarchy of the LO, NLO and NNLO contributions, we can set $\mu_F=\mu_R=M_H=115\,\text{GeV}$ and $\alpha_S(M_H)=0.112$. The first three terms in the expansion (2.7) thus give

$$
\begin{aligned}
G_{gg}^{\text{SV}}(z)=\alpha_S^2\Big\{&\delta(1-z)\,(1+0.548+0.105)+\mathcal{D}_0\,(0+0+0.283)+\\
&+\mathcal{D}_1\,(0+0.428-0.040)+\mathcal{D}_2\,(0+0-0.029)+\mathcal{D}_3\,(0+0+0.092)\Big\}.
\end{aligned}
$$

Since $1\geq z=\tau_H/\tau\geq\tau_H$, the SV terms are certainly the dominant contributions to the cross section in the kinematic region near the hadronic threshold ($\tau_H=M_H^2/s\sim 1$). At fixed s, this means that these terms certainly dominate in the case of heavy Higgs bosons. However, the SV terms can give the dominant effect even long before the threshold region in the hadronic cross section is actually approached [30]. This is because, in the evaluation of the hadronic cross section in eq. (2.3), the partonic cross section $\hat{\sigma}_{ab}(\hat{s},M_H^2)$ has to be weighted with the parton luminosities, which are strongly suppressed at large $\tau=\hat{s}/s=x_1x_2$. In other words, owing to the strong suppression of the parton densities $f_a(x,\mu_F^2)$ at large x, the partonic centre-of-mass energy $\sqrt{\hat{s}}$ is typically substantially smaller than $\sqrt{s}$ ($\langle\hat{s}\rangle=\langle x_1x_2s\rangle=\langle\tau\rangle s$), and the variable $z=M_H^2/\hat{s}$ in $G_{ab}(z)$ can be close to unity also when $\sqrt{s}$ is not very close to M_H.

At fixed M_H, the quantitative reliability of the large-z approximation depends on the value of $\sqrt{s}$ and on the actual value of the parton luminosities $\mathcal{L}_{ab/h_1h_2}(\tau,\mu_F^2)$ in eq. (2.3). In figure 1 the gg and $(qg+g\bar{q})$ luminosities (with $\mu_F=M_H=150\,\text{GeV}$) at the Tevatron Run II are plotted as a function of the partonic centre-of-mass energy $\sqrt{\hat{s}}$ ($\hat{s}=\tau s$). We see that the luminosities decrease by almost two orders of magnitude when $\sqrt{\hat{s}}$ increases from $M_H=150\,\text{GeV}$ (hadronic threshold) to $300\,\text{GeV}$. A similar effect occurs at the LHC (see figure 1 in ref. [26]). We thus expect that the large-z expansion of the coefficient function $G_{ab}(z)$ reliably approximates the size of the higher-order QCD corrections to Higgs boson production at the Tevatron and the LHC. At NLO, this was explicitly checked in ref. [15], by comparison with the complete expression of $G_{ab}^{(1)}(z)$.

The authors of ref. [15] also pointed out that at NLO the numerical effect of the logarithmic term $\ln(1-z)$ of collinear origin is not small. Following this observation, in ref. [16] we introduced the soft-virtual-collinear (SVC) approximation of the coefficient function $G_{ab}(z)$. The SVC approximation is defined by including the leading $\ln^k(1-z)$ contribution from the collinear region in the gg channel:

$$
G_{gg}^{(1)\text{SVC}}\left(z;\frac{M_H^2}{\mu_R^2};\frac{M_H^2}{\mu_F^2}\right)=G_{gg}^{(1)\text{SV}}\left(z;\frac{M_H^2}{\mu_R^2};\frac{M_H^2}{\mu_F^2}\right)-12\,\ln(1-z)\,, \qquad (2.12)
$$

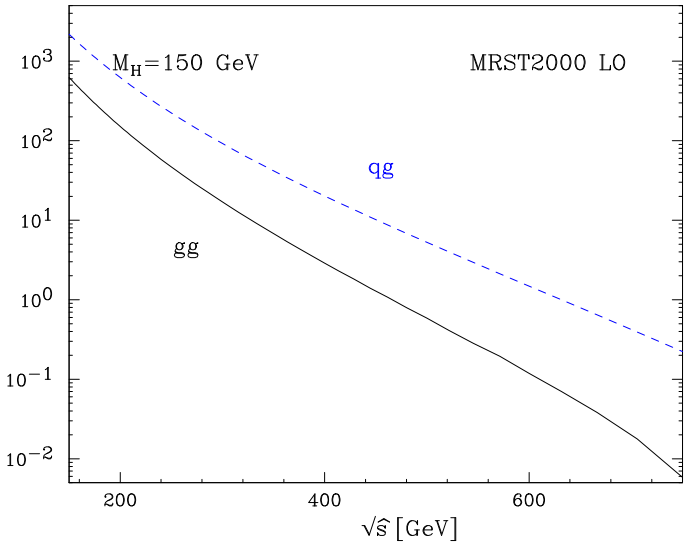

Figure 1: Parton (gg and $qg+g\bar{q}$) luminosities $\mathcal{L}(\tau,\mu_F^2)$ with $\mu_F = M_H = 150\,\mathrm{GeV}$ at the Tevatron Run II as a function of the partonic centre-of-mass energy $\sqrt{\hat{s}}$ ($\hat{s}=\tau s$). We use the LO set of parton distributions in ref. [24].

$$G_{gg}^{(2)\mathrm{SVC}}\left(z;\frac{M_H^2}{\mu_R^2};\frac{M_H^2}{\mu_F^2}\right) = G_{gg}^{(2)\mathrm{SV}}\left(z;\frac{M_H^2}{\mu_R^2};\frac{M_H^2}{\mu_F^2}\right) - 72\,\ln^3(1-z)\,. \tag{2.13}$$

Since the term $\ln^k(1-z)$ added to the SV expressions is that with the highest power k at each perturbative order ($k=1$ and $k=3$ at LO and NLO, respectively), the SVC approximation consistently includes the next-to-dominant contribution to $G_{gg}^{(2)}$ in the limit $z\to 1$. The comparison between the SV and the SVC approximations can thus be used [16] to gauge the quantitative accuracy of approximating $G_{ab}(z)$ by its large-z limit. In the next section we study the impact of the SV and SVC approximations at the Tevatron Run II.

Two different large-z approximations, named 'soft' and 'soft+sl' were also considered in the numerical study of ref. [17]. The 'soft' approximation of ref. [17] regards the whole partonic cross section $\hat{\sigma}_{ab}$ in eq. (2.2), while our SV approximation refers only to the hard coefficient function $G_{ab}(z)$. In other words, we perform the soft approximation on the phase-space integral of the matrix elements squared, while the *kinematical* flux factor $1/\hat{s}$ in $\hat{\sigma}_{ab}$ is kept fixed and not expanded around $\hat{s}=s$. This means that we expand $G_{ab}(z)$ around $z=1$, whereas the authors of ref. [17] consider the expansion of $\widetilde{G}_{ab}(z) = zG_{ab}(z)$. Owing to the identity

$$z\,\mathcal{D}_i = \mathcal{D}_i - \ln^i(1-z)\,, \tag{2.14}$$

the two expansions differ by subdominant $\ln^i(1-z)$ contributions of kinematical origin (see also section 3 in ref. [16]). Moreover, the 'soft+sl' approximation of $\widetilde{G}_{gg}^{(2)}$ [17] includes also additional subleading terms, proportional to $\ln^2(1-z)$ and $\ln(1-z)$, whose coefficients (unlike those in eqs. (2.11) and (2.13)) are not (exactly) predictable at present [15]. In summary, we note that there is no one-to-one correspondence between 'soft' (or 'soft+sl') in ref. [17] and SV (or SVC) in our definition, the difference being due to logarithmic contributions that, formally, are consistently subdominant when $z\to 1$.

Although, from a formal viewpoint, it is legitimate to perform the large-z expansion of either $G_{ab}(z)$ or $\widetilde{G}_{ab}(z)$, the two expansions can quantitatively differ when applied to the evaluation of the hadronic cross section in eq. (2.1). In fact, when using $\widetilde{G}_{ab}(z)$, the analogue of eq. (2.3) is

$$\sigma(s, M_H^2) = \sigma_0 \sum_{a,b} \int_{\tau_H}^1 \frac{d\tau}{\tau}\, \widetilde{\mathcal{L}}_{ab/h_1h_2}(\tau, \mu_F^2)\, \widetilde{G}_{ab}(\tau_H/\tau)\,. \tag{2.15}$$

Comparing eqs. (2.3) and (2.15), we see that the coefficient function $\widetilde{G}_{ab}(z = \tau_H/\tau)$ is convoluted with the momentum-fraction luminosity $\widetilde{\mathcal{L}}(\tau, \mu_F^2) = \tau \mathcal{L}(\tau, \mu_F^2)$. Owing to the relative rescaling factor $\tau = \hat{s}/s$, $\widetilde{\mathcal{L}}(\tau, \mu_F^2)$ is much less steep than the luminosity $\mathcal{L}(\tau, \mu_F^2)$ (see figure 1) that enters eq. (2.3). Therefore, in the numerical evaluation of the Higgs boson cross section, we expect and anticipate (see the comment at the end of section 3) that the large-z expansion of $\widetilde{G}_{ab}(z)$ [15, 17] converges more slowly than that of $G_{ab}(z)$. The slowing down is ultimately caused by a too extreme kinematics approximation of the partonic cross section in eq. (2.2): the flux factor $1/\hat{s}$ has been replaced by $1/M_H^2$.

3. Inclusive production at the Tevatron Run II

In this section we study the higher-order QCD corrections to the inclusive production of the SM Higgs boson at the Tevatron Run II, i.e. proton-antiproton collisions at $\sqrt{s} = 2\,\text{TeV}$. We recall that we include the exact dependence on M_{top} in the Born-level cross section σ_0 (see eq. (2.5)), while the coefficient function $G_{ab}(z)$ is evaluated in the large-M_{top} limit. At NLO [14, 15] this is a very good numerical approximation when $M_H \leq 2M_{\text{top}}$.

Unless otherwise stated, cross sections are computed using the MRST2000 [24] sets of parton distributions with densities and coupling constant evaluated at each corresponding order, i.e. using LO distributions and 1-loop α_S for the LO cross section, and so forth. The corresponding values of $\Lambda^{(5)}_{QCD}$ ($\alpha_S(M_Z)$) are 0.132 (0.1253), 0.22 (0.1175) and 0.187 (0.1161) GeV, at 1-loop, 2-loop and 3-loop order, respectively. In the NNLO case we use the 'central' set of MRST2000, obtained from a global fit of data (deep inelastic scattering, Drell-Yan production and jet E_T distribution) by using the approximate NNLO evolution kernels presented in ref. [25]. The result we refer to as NNLO-SV(SVC) corresponds to the sum of the LO and exact NLO (including the qg and $q\bar{q}$ channels) contributions plus the SV(SVC) corrections at NNLO, given in eq. (2.11) (eq. (2.13)).

In figure 2 we show the dependence of the LO and NLO cross sections on the choice of parton distributions. The results obtained by using both the GRV98 [31] and CTEQ5 [32] sets differ substantially from the MRST2000 results. In the case of the GRV98 sets, this difference is not unexpected, since the value of $\alpha_S(M_Z)$ and the gluon distribution are quite different from those of MRST2000 and CTEQ5. We see that, as M_H increases from 100 to 200 GeV, the LO result obtained by using the CTEQ5 set is between 10 and 30% lower than the one obtained by MRST2000. At NLO the difference is smaller, and it is compatible with the $\pm 10\%$ uncertainty recommended by the CTEQ collaboration [33] on gg and qg luminosities in the x region that controls Higgs boson production at the Tevatron.

JHEP01(2002)015

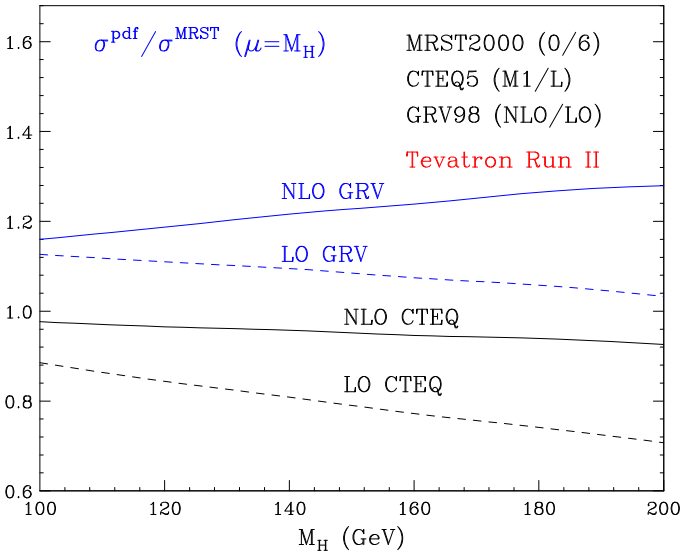

Figure 2: Relative difference of LO and NLO results computed with GRV98 and CTEQ5 distributions with respect to MRST2000 distribution.

Although the LO differences are physically less meaningful than the NLO differences, the size of the former has to be kept in mind when quoting QCD predictions (based on either analytic calculations or Monte Carlo event generators) that directly or indirectly (e.g. in the case of K-factors) use LO parton densities.

Figure 3 shows the scale dependence of the cross section for the production of a Higgs boson with $M_H = 150\,\text{GeV}$. The scale dependence is analysed by varying the factorization and renormalization scales by a factor of 4 up and down from the central value M_H. The plot on the left corresponds to the simultaneous variation of both scales, $\mu_F = \mu_R = \chi\, M_H$, whereas the plots in the centre and on the right respectively correspond to the results of the independent variation of the factorization and renormalization scales, keeping the other fixed at the central value.

As expected from the QCD running of α_S, the cross sections typically decrease when μ_R increases around the characteristic hard scale M_H. A similar behaviour[3] is observed when μ_F varies, since the cross sections are mainly sensitive to partons with momentum fraction $x \sim 0.05$–0.1, and in this x range scaling violation of the parton densities is (slightly) negative. The largest variations in the cross section calculation are thus obtained by simultaneously varying μ_R and μ_F. The scale dependence is mostly driven by the renormalization scale, because the lowest-order contribution to the process is proportional to α_S^2, a (relatively) high power of α_S.

In summary, figure 3 shows that the scale dependence is reduced when higher-order corrections are included. Varying the scales in the range $0.5 \leq \chi_R, \chi_F \leq 2$, the reduction is from about $\pm 20\%$ at full NLO to about $\pm 10\%$ and $\pm 15\%$ at NNLO-SV and NNLO-SVC, respectively. The increase in the scale dependence when going from NNLO-SV to NNLO-SVC is due to the fact that the contribution of the dominant collinear terms included in

[3] At the LHC, the μ_F dependence is opposite, as shown in figure 1 of ref. [16].

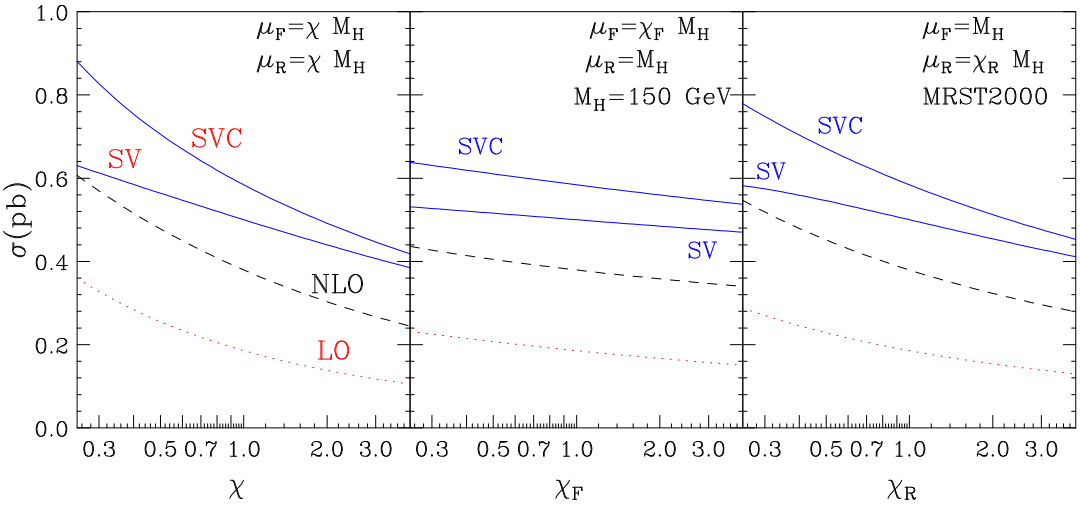

Figure 3: Scale dependence of the Higgs production cross section for $M_H = 150\,\text{GeV}$ at LO, NLO, NNLO-SV and NNLO-SVC.

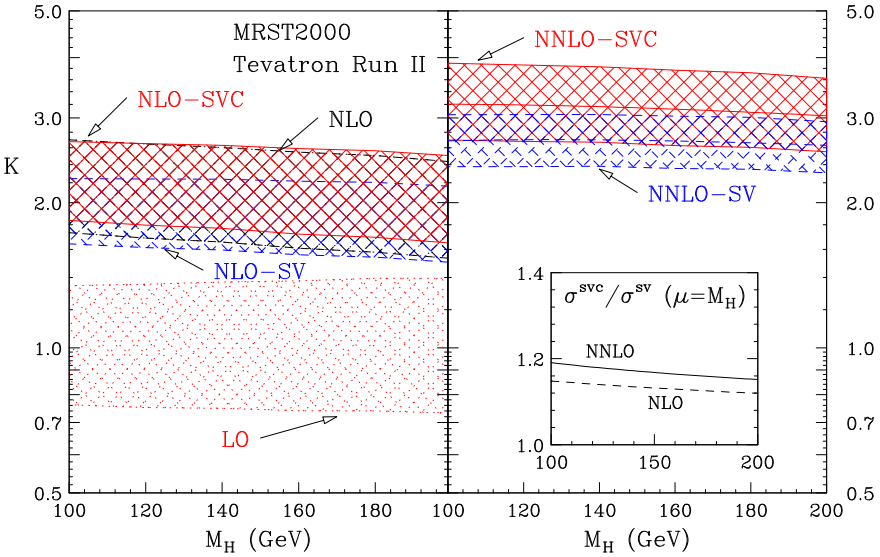

Figure 4: K-factors for Higgs production for the full NLO result and the NLO-SV, NLO-SVC, NNLO-SV and NNLO-SVC approximations.

the SVC approximation (see eqs. (2.12) and (2.13)) is not small and scale-independent, so it cannot be compensated by scale variations.

In figure 4 we study the K-factors, defined as the ratio of the cross section evaluated at each corresponding order over the LO result. Since the LO result sizeably depends on the choice of parton distributions, the K-factor should be interpreted with care. For instance, for $M_H = 180\,\text{GeV}$, the NLO K-factor computed by using MRST distributions is about 20% smaller than the one obtained by using CTEQ distributions.

In figure 4 the bands account for the 'theoretical uncertainty' due to the scale dependence, quantified by using the minimum and maximum values of the cross sections when

JHEP01(2002)015

the scales μ_R and μ_F are varied (simultaneously and independently, as in figure 3) in the range $0.5 \leq \chi_R, \chi_F \leq 2$. The LO result that normalizes the K-factors is computed at the default scale M_H in all cases.

The plot on the left-hand side of figure 4 shows the scale uncertainty at LO and compares the full NLO result with the NLO-SV and NLO-SVC approximations. When M_H is in the range 140–180 GeV, the NLO-SV approximation tends to underestimate the full NLO result by about 7–8%, whereas the NLO-SVC approximation overestimates it by about 4–5%, showing the effect of the term $\ln(1-z)$ added in the SVC approximation. We find that the SVC result provides an excellent approximation of the full gg contribution at NLO, the difference being less than 2 per mille. The contribution of the qg channel tends to lower the SVC result by $\lesssim 5\%$. The effect of the qg channel is mainly due to the logarithmically-enhanced behaviour $G_{qg}^{(1)}(z) \simeq \frac{4}{3}\ln(1-z)$ of the corresponding coefficient function at large z. The improved reliability of the SV and SVC approximations with respect to the LHC [16] is not unexpected since at the Tevatron we are closer to threshold.

The right-hand side of figure 4 shows the SV and SVC results at NNLO. Again, the SVC band sits higher than the SV one and, as shown in the inset plot, the ratio of the corresponding cross sections increases with respect to NLO. The contribution from non-leading terms $\ln^k(1-z)$, with $k < 3$ (which are not under control within the SVC approximation), is not included. We have tried to add a term $\ln^2(1-z)$ with a coefficient as large as the one of the $\ln^3(1-z)$ contribution, and we have found a small ($\mathcal{O}(5\%)$) modification. Therefore, we expect the effect of these non-leading logarithmic terms to be numerically less important. As pointed out in ref. [16], at NNLO there is a (still unknown) leading collinear contribution proportional to $\ln^3(1-z)$ also in the qg channel. Owing to the size of the contribution of the qg channel at NLO, the quantitative effect of this NNLO term can be of the same order as the corresponding one included through the SVC approximation in the gg channel.

We recall that the NNLO results on the right-hand side of figure 4 are obtained by using the (approximated) NNLO parton distributions of the MRST2000 set. Using the NLO parton distributions, the K-factors would be smaller by about 5 to 8% as M_H increases from 120 to 180 GeV.

In summary, considering the results obtained at NLO, we expect the full NNLO K-factor to be between the SV and SVC bands. For reference, we give in Table 1 the central values of the cross section in the range $M_H = 140$–180 GeV. In particular, for a light Higgs boson ($M_H \lesssim 200$ GeV), this corresponds to an increase of about 50% with respect to the full NLO result, i.e. a factor of ~ 3 with respect to the LO result. Taking into account that the NLO result increases the LO cross section by a factor of about 2, our result shows that the convergence of the perturbative series is poorer at the Tevatron than at the LHC [16]. This also implies that QCD contributions beyond NNLO can still be significant at the Tevatron.

Our conclusion on the possible relevance of higher-order contributions is not in contradiction with the improved scale dependence of the NNLO calculation. As is well known, the customary procedure of varying the scales to estimate the theoretical uncertainty due

JHEP01(2002)015

M_H(GeV)	LO	NLO	NLO-SV	NLO-SVC	NNLO-SV	NNLO-SVC
140	0.2282	0.4715	0.4338	0.4922	0.6163	0.7222
150	0.1856	0.3794	0.3507	0.3969	0.5002	0.5841
160	0.1523	0.3080	0.2859	0.3229	0.4092	0.4763
170	0.1260	0.2519	0.2349	0.2646	0.3369	0.3912
180	0.1050	0.2075	0.1943	0.2184	0.2795	0.3235

Table 1: Cross sections in pb as a function of M_H. The calculation is performed by setting $\mu_R = \mu_F = M_H$.

to missing higher-order terms can only give a lower limit on the 'true' uncertainty. This is well demonstrated by the plot on the left-hand side of figure 4, which shows no overlap between the LO and NLO bands. Since the NLO and NNLO bands still tend to show no (or a marginal) overlap, their size cannot yet be regarded as a reliable estimate of the theoretical uncertainty.

A comment on the numerical results presented in ref. [17] is in order. The authors of ref. [17] use different parton distributions and, as explained in section 2, there is no one-to-one correspondence between their 'soft' (or 'soft+sl') approximation and our SV (or SVC) approximation. Therefore, those results cannot directly be compared with ours (see also ref. [34]). Certainly, they show a slower numerical convergence of the large-z expansion used in ref. [17]. As discussed at the end of section 2, this is not unexpected because of significant subdominant effects of kinematical origin.

4. Vetoed cross section

Direct Higgs production followed by the decay $H \to WW \to l^+ l^- \nu\bar{\nu}$ is an important channel to discover the SM Higgs boson in the intermediate-mass range $140\,\text{GeV} \lesssim M_H \lesssim 190\,\text{GeV}$ both at the Tevatron and at the LHC. Nevertheless, as recalled in section 1, several experimental cuts have to be applied to discriminate the signal over the background. An important selection to enhance the statistical significance is a veto on the high transverse-momentum jets that accompany the production of the Higgs boson. Events with high transverse-momentum jets are excluded from the analysis [6, 7, 11].

In this section we study the effect of a jet veto on inclusive Higgs production. The events that pass the veto selection are those with $p_T^{\text{jet}} < p_T^{\text{veto}}$, where p_T^{jet} is the transverse momentum of any final-state jets. Jets are defined by a cone algorithm. In the perturbative calculation, jets are represented by a parton or a set of partons. The Higgs boson can be accompanied by one final-state parton at NLO, and by one or two final-state partons at NNLO. In the case of a single final-state parton with transverse momentum $\mathbf{p}_{1\,T}$, the vetoed cross section is computed by imposing $|\mathbf{p}_{1\,T}| < p_T^{\text{veto}}$ (i.e. we veto events with $|\mathbf{p}_{1\,T}| > p_T^{\text{veto}}$). When there are two final-state partons with transverse momenta $\mathbf{p}_{1\,T}$ and $\mathbf{p}_{2\,T}$, we consider their angular distance $R_{12}^2 = (\eta_1 - \eta_2)^2 + (\phi_1 - \phi_2)^2$ in the pseudorapidity-azimuth plane: if $R_{12} > R$, we impose the constraints $|\mathbf{p}_{1\,T}|, |\mathbf{p}_{2\,T}| < p_T^{\text{veto}}$ (i.e. we veto events with $|\mathbf{p}_{1\,T}| > p_T^{\text{veto}}$ or $|\mathbf{p}_{2\,T}| > p_T^{\text{veto}}$); if $R_{12} < R$, we combine the two partons in a

single jet and we impose $|\mathbf{p}_{1\,T}+\mathbf{p}_{2\,T}| < p_T^{\rm veto}$ (i.e. we veto events with $|\mathbf{p}_{1\,T}+\mathbf{p}_{2\,T}| > p_T^{\rm veto}$). In all the numerical results presented in this section, the cone size R of the jets is fixed at the value $R = 0.4$.

As in the case of the inclusive cross section, we evaluate the jet-vetoed cross section by using the large-$M_{\rm top}$ limit. Studies on Higgs+jets production show that the QCD matrix elements in the large-$M_{\rm top}$ limit [35, 36] approximate very well those with the exact $M_{\rm top}$ dependence [37, 38], provided the jet transverse momenta and, hence, $p_T^{\rm veto}$ remain small with respect to $M_{\rm top}$.

The vetoed cross section $\sigma^{\rm veto}(s, M_H^2; p_T^{\rm veto}, R)$ can be written as

$$\sigma^{\rm veto}(s, M_H^2; p_T^{\rm veto}, R) = \sigma(s, M_H^2) - \Delta\sigma(s, M_H^2; p_T^{\rm veto}, R)\,, \tag{4.1}$$

where $\sigma(s, M_H^2)$ is the inclusive hadronic cross section in eq. (2.1), and $\Delta\sigma$ is the 'loss' in cross section due to the jet-veto procedure. The vetoed cross section is computable by a factorization formula analogous to eq. (2.1), apart from the replacement of the coefficient function $G_{ab}(z)$ by the vetoed coefficient function $G_{ab}^{\rm veto}(z; \pi_T, R)$. By analogy with eq. (4.1), we can write the vetoed coefficient function as

$$G_{ab}^{\rm veto}(z; \pi_T, R) = G_{ab}(z) - \Delta G_{ab}(z; \pi_T, R)\,, \tag{4.2}$$

where, to simplify the notation (see eq. (4.5)), the dependence on $p_T^{\rm veto}$ is parametrized by the dimensionless variable π_T:

$$\pi_T\left(z, \frac{p_T^{\rm veto}}{M_H}\right) \equiv \frac{2p_T^{\rm veto}\sqrt{z}}{(1-z)M_H}\,. \tag{4.3}$$

At LO, the vetoed cross section is equal to the inclusive one, so the subtracted coefficient function ΔG_{ab} vanishes. At higher perturbative orders, ΔG_{ab} is computable according to the power-series expansion

$$\begin{aligned}\Delta G_{ab}\left(z; \pi_T, R; \alpha_{\rm S}(\mu_R^2), \frac{M_H^2}{\mu_R^2}; \frac{M_H^2}{\mu_F^2}\right) = \frac{\alpha_{\rm S}^3(\mu_R^2)}{\pi}\Delta G_{ab}^{(1)}\left(z; \pi_T\right)\Theta\left(1 - \pi_T\left(z, \frac{p_T^{\rm veto}}{M_H}\right)\right) + \\ + \frac{\alpha_{\rm S}^4(\mu_R^2)}{\pi^2}\,\Delta G_{ab}^{(2)}\left(z; \pi_T, R; \frac{M_H^2}{\mu_R^2}; \frac{M_H^2}{\mu_F^2}\right) + \mathcal{O}(\alpha_{\rm S}^5)\,.\end{aligned} \tag{4.4}$$

The NLO contribution $\Delta G_{ab}^{(1)}$ is scale-independent and R-independent, but it depends on $p_T^{\rm veto}$. We have explicitly evaluated it in the large-$M_{\rm top}$ limit, and we find:

$$\begin{aligned}\Delta G_{gg}^{(1)}(z; \pi_T) &= \hat{P}_{gg}(z)\,\ln\frac{1+\sqrt{1-\pi_T^2}}{1-\sqrt{1-\pi_T^2}} - \frac{11}{2}\,\frac{(1-z)^3}{z}\left(1-\frac{\pi_T^2}{22}\right)\sqrt{1-\pi_T^2}\,,\\
\Delta G_{gq}^{(1)}(z; \pi_T) &= \frac{1}{2}\hat{P}_{gq}(z)\,\ln\frac{1+\sqrt{1-\pi_T^2}}{1-\sqrt{1-\pi_T^2}} - \frac{(1-z)^2}{z}\sqrt{1-\pi_T^2}\,,\\
\Delta G_{q\bar{q}}^{(1)}(z; \pi_T) &= \frac{32}{27}\,\frac{(1-z)^3}{z}\left(1-\frac{\pi_T^2}{4}\right)\sqrt{1-\pi_T^2}\,,\end{aligned} \tag{4.5}$$

where

$$\hat{P}_{gq}(z) = \frac{4}{3}\,\frac{1+(1-z)^2}{z}\,,$$
$$\hat{P}_{gg}(z) = 6\left[\frac{1-z}{z} + \frac{z}{1-z} + z(1-z)\right]. \qquad (4.6)$$

The evaluation of the NNLO contribution $\Delta G_{ab}^{(2)}$ cannot be easily performed in analytic form, since the calculation depends on the details of the jet algorithm. We compute $\Delta G_{ab}^{(2)}$ numerically by using the program of ref. [27]. The program, which implements the matrix elements (in the large-$M_{\rm top}$ limit) of refs. [35, 36] by using the subtraction-method procedure of ref. [39], computes the QCD corrections to Higgs+jet(s) production up to order $\alpha_{\rm S}^4$. For the purpose of evaluating the contribution $\Delta\sigma$ to eq. (4.1), we use the program to compute the Higgs+jet(s) cross section when the transverse momentum of the highest-p_T jet is larger than $p_T^{\rm veto}$.

In the following we present both NLO and NNLO numerical results for the vetoed cross section $\sigma^{\rm veto}$ in eq. (4.1). The results are obtained by using the parton distributions of the MRST2000 set, as explained in section 3. The NLO calculation is exact: apart from using the large-$M_{\rm top}$ limit, we do not perform any further approximations. At the NNLO, the contribution $\Delta\sigma$ to eq. (4.1) is again evaluated exactly, while to evaluate the contribution of the inclusive cross section we rely on our approximate estimate in section 3 (see the corresponding LHC results in section 4 of ref. [16]) and, in particular, we use the NNLO-SVC result. Therefore, once the full NNLO result for the inclusive cross section is available, it can straightforwardly be used to 'correct' our NNLO estimate for the vetoed cross section. As stated above, in our numerical calculations we fixed the cone size of the jets to the value $R = 0.4$. The R-dependence of the perturbative calculation first appears at the NNLO. In particular, the NNLO vetoed cross section decreases by increasing R.

Note that the numerical program of ref. [27] is a Monte Carlo code that evaluates Higgs+jet(s) production at the fully exclusive level. Therefore, it can be used through the subtraction procedure of eq. (4.1) to compute vetoed cross sections also when additional kinematical cuts (e.g. cuts on the rapidities of the jets, or asymmetric cuts on the jet transverse momenta) or different jet definitions are considered.

We first present the vetoed cross section[4] at the Tevatron Run II. In figure 5 we show the dependence of the NLO results on the Higgs mass for different values of $p_T^{\rm veto}$ (15, 20, 30 and 50 GeV). The vetoed cross sections $\sigma^{\rm veto}(s, M_H^2; p_T^{\rm veto}, R)$ and the inclusive cross section $\sigma(s, M_H^2)$ are given in the plot on the left-hand side. The inset plot gives an idea of the 'loss' in cross section once the veto is applied, by showing the ratio between the cross section difference $\Delta\sigma$ in eq. (4.1) and the inclusive cross section at the same perturbative order. As can be observed, for large values of the cut, say $p_T^{\rm veto} = 50\,{\rm GeV}$, less than 10%

[4]The numerical program of ref. [27] implements the large-$M_{\rm top}$ limit strictly, i.e. also the Born-level contribution σ_0 in eq. (2.5) is evaluated in the limit $M_H/M_{\rm top} \to 0$. For simplicity, the numerical results of this section implement the same approximation. The approximation used in section 3 can be recovered by simply rescaling the absolute value of the cross sections by the overall factor $\sigma_0/\sigma_0(M_H/M_{\rm top} = 0)$. Of course, such a rescaling has no effects on the ratios $\Delta\sigma/\sigma$ and on the vetoed K-factors.

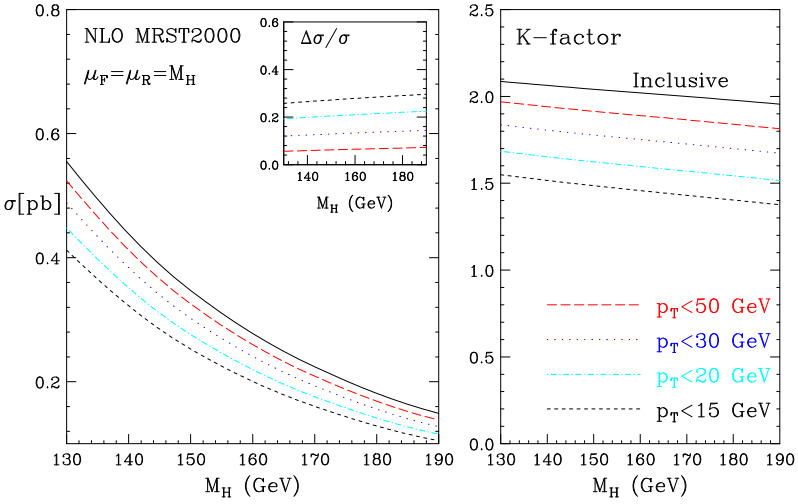

Figure 5: Vetoed cross section and K-factors: NLO results at the Tevatron Run II.

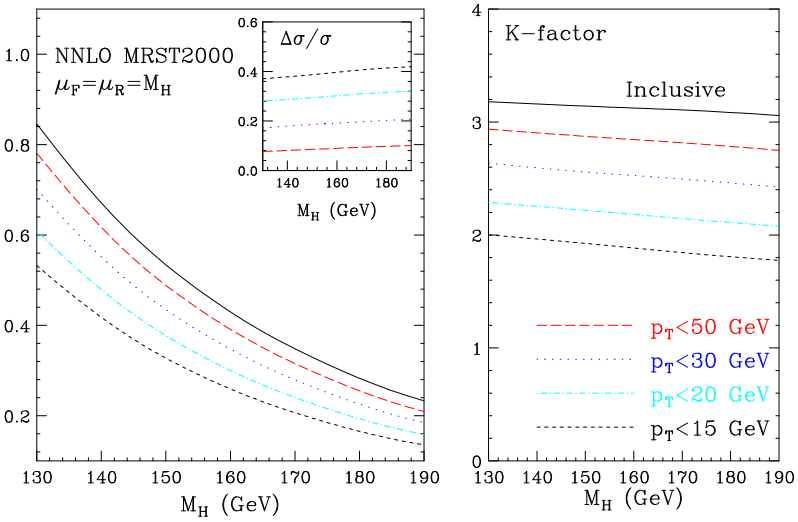

Figure 6: Vetoed cross section and K-factors: NNLO results at the Tevatron Run II.

of the inclusive cross section is vetoed. The veto effect increases by decreasing $p_T^{\rm veto}$, but it is still smaller than 30% when $p_T^{\rm veto} = 15\,\text{GeV}$. On the right-hand side of figure 5, we show the corresponding K-factors, i.e. the vetoed cross sections normalized to the LO result, which is independent of the value of the cut.

Figure 6 shows the analogous results at NNLO. Note that, although $\Delta\sigma/\sigma$ is slightly larger than at NLO, the vetoed cross sections and, thus, the K-factors, are still larger than at NLO. This is mostly due to the large increase of the inclusive cross section at NNLO, as shown in section 3.

All the results plotted in figures 5 and 6 have been obtained by fixing the renormalization and factorization scales at the default value $\mu_R = \mu_F = M_H$. In figure 7, we study the scale dependence of the cross sections (inclusive and with $p_T^{\rm veto} = 15$ and $30\,\text{GeV}$) at LO,

JHEP01(2002)015

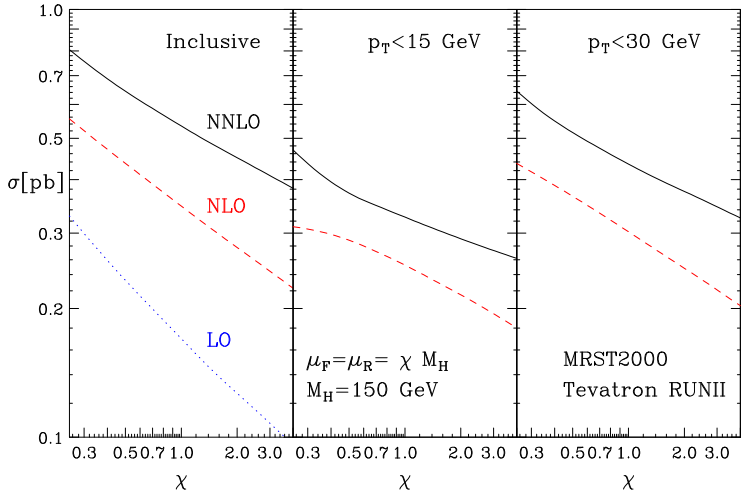

Figure 7: Scale dependence of the inclusive and vetoed cross sections at LO, NLO and NNLO-SVC at the Tevatron.

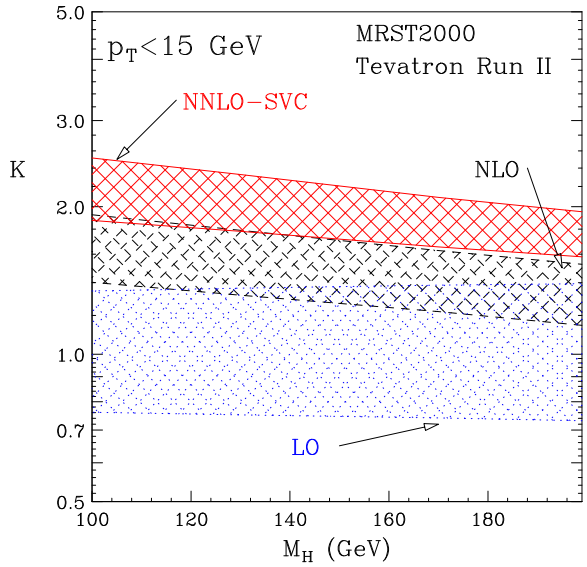

Figure 8: K-factors for Higgs production at the Tevatron in the case of a veto of $p_T^{\rm veto} = 15\,\text{GeV}$: LO, NLO and NNLO-SVC approximation.

NLO and NNLO. The renormalization and factorization scales are varied simultaneously by a factor of 4 up and down with respect to M_H. No significant differences are found when the scales are varied separately. As can be observed, there is an improvement in the stability of the result when higher order corrections are included. This is particularly noticeable when going from LO to NLO, while the comparison between NNLO and NLO looks rather similar to the one observed in the inclusive case.

The scale-dependence effects on the perturbative K-factors can be appreciated also from figure 8, where the LO, NLO and NNLO-SVC bands (computed as in figure 4) are shown in the case in which a veto of $p_T^{\rm veto} = 15\,\text{GeV}$ is applied. Comparing figure 8 with

JHEP01(2002)015

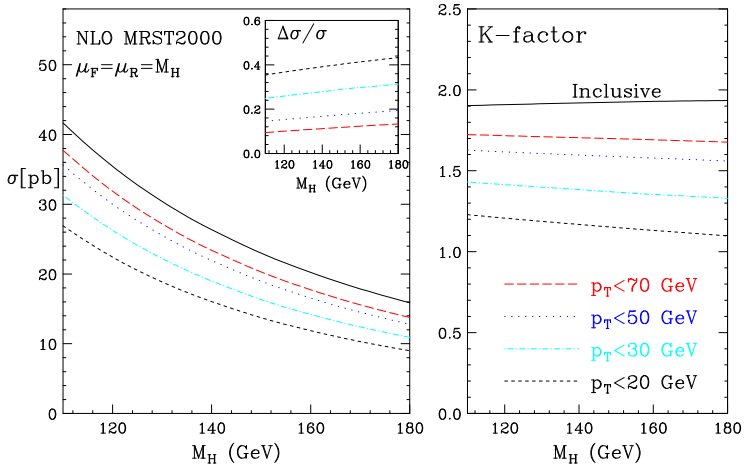

Figure 9: Vetoed cross sections and K-factors at NLO at the LHC.

the inclusive case in figure 4, we see that the effect of the veto is to partially reduce the relative difference between the NLO and NNLO results; the increase of the corresponding K-factors can be estimated to about 25%.

The results on the jet veto presented so far can be qualitatively explained by a simple physical picture. As shown in section 3, the effect of the higher-order contributions to inclusive Higgs boson production at the Tevatron is large. The dominant part of this effect is due to soft and collinear radiation, whereas the accompanying hard radiation has little effect. The characteristic scale of the highest transverse momentum $p_T^{\max}$ of the accompanying jets is indeed $p_T^{\max} \sim \langle 1-z\rangle M_H$ (see e.g. the upper bound on $p_T^{\rm veto}$ from the theta function in eq. (4.4)), where the average value $\langle 1-z\rangle = \langle 1 - M_H^2/\hat{s}\rangle$ of the distance from the partonic threshold is small. As a consequence the jet veto procedure is weakly effective unless the value of $p_T^{\rm veto}$ is pretty small (i.e. substantially smaller than $p_T^{\max}$). Decreasing $p_T^{\rm veto}$, the enhancement of the inclusive cross section due to soft radiation at higher orders is reduced, and the jet veto procedure tends to improve the convergence of the perturbative series (see e.g. figures 4 and 8). Note also that the characteristic scale $p_T^{\max}$ is a slightly increasing function of M_H, the linear increase with M_H being partially compensated by the decrease of $\langle 1-z\rangle$. Therefore, at fixed $p_T^{\rm veto}$ the vetoed K-factor decreases more than the inclusive K-factor when M_H increases (see figure 6).

On the basis of this physical picture, we can easily anticipate the qualitative effect of the jet veto at the LHC. The overall features of the QCD corrections to inclusive Higgs boson production at the LHC [16] are the same as at the Tevatron. The main quantitative differences arise from the fact that Higgs production at the LHC is less close to threshold than at the Tevatron and, therefore, the accompanying jets are less soft ($\langle 1-z\rangle$ is larger) at the LHC than at the Tevatron. At fixed $p_T^{\rm veto}$ the effect of the jet veto is thus stronger at the LHC.

The results for the vetoed cross sections at the LHC are presented in figures 9 and 10 for $p_T^{\rm veto} = 20$, 30, 50 and 70 GeV. In figures 11 and 12, we show the perturbative K-factors and their scale dependence for two representative values, $p_T^{\rm veto} = 30\,\text{GeV}$ and $p_T^{\rm veto} = 15\,\text{GeV}$, of

JHEP01(2002)015

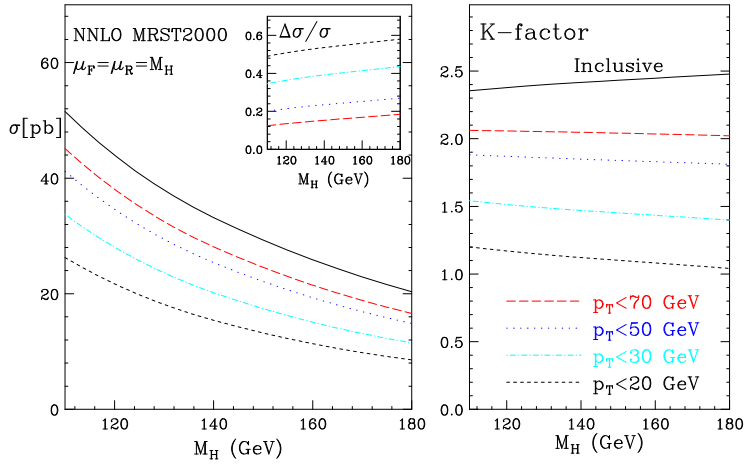

Figure 10: Vetoed cross sections and K-factors at NNLO at the LHC.

the transverse-momentum veto. At fixed value of the cut, the impact of the jet veto, both in the 'loss' of cross section and in the reduction of the K-factors, is larger at the LHC than at the Tevatron Run II. This effect can also be appreciated by comparing figure 11 and figure 8. At the LHC, the value of $p_T^{\rm veto} = 30\,{\rm GeV}$ is already sufficient to reduce the difference between the NNLO and NLO results to less than 10%. This better apparent convergence of the perturbative expansion is consistent with the fact that the scale-dependence bands overlap more in figure 11 than in figure 8 (see also figure 2 in ref. [16], which shows the scale dependence of the inclusive K-factor at the LHC).

Note that when $p_T^{\rm veto}$ is much smaller than the characteristic scale $p_T^{\rm max} \sim \langle 1-z\rangle M_H$, the coefficients of the perturbative expansion of the vetoed cross section contain large logarithmically-enhanced contributions. For instance, from eq. (4.5) we have

$$\Delta G_{gg}^{(1)}(z;\pi_T) \sim 2\hat{P}_{gg}(z)\,\ln\frac{(1-z)M_H}{p_T^{\rm veto}}\,. \tag{4.7}$$

The presence of these contributions can spoil the quantitative convergence of the fixed-order expansion in α_S. Since $\langle 1-z\rangle M_H$ is larger at the LHC than at the Tevatron, the value of $p_T^{\rm veto}$ at which these effects become visible is larger at the LHC. The perturbative K-factors shown in figure 12 suggest that at the LHC the vetoed cross section is sensitive to these large logarithmic terms already when $p_T^{\rm veto} = 15\,{\rm GeV}$. Indeed, the scale-dependence band is larger at NNLO than at NLO. At such small values of $p_T^{\rm veto}$, perturbative contributions beyond the NNLO can still be significant.

5. Conclusions

In this paper we have presented our study of QCD radiative corrections to direct Higgs boson production at hadron colliders and the impact of jet veto.

Using the theoretical results of refs. [16, 17], in section 3 we have first shown that the NNLO-SV and NNLO-SVC approximations are expected to be a good estimate of the full NNLO contributions to the inclusive cross section at the Tevatron Run II. Similar

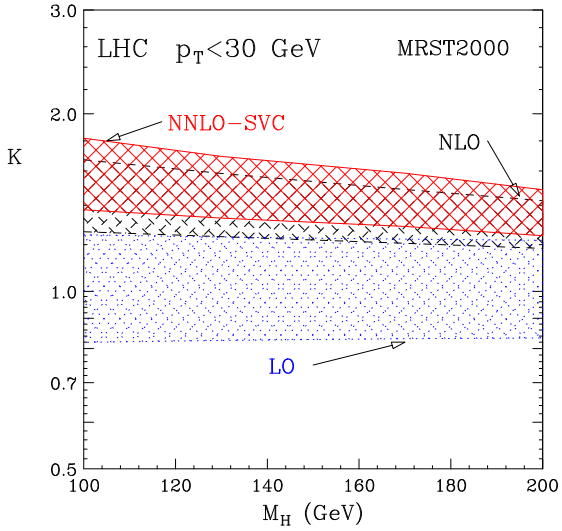

Figure 11: The same as in figure 8, but at the LHC and with $p_T^{cut} = 30\,\text{GeV}$.

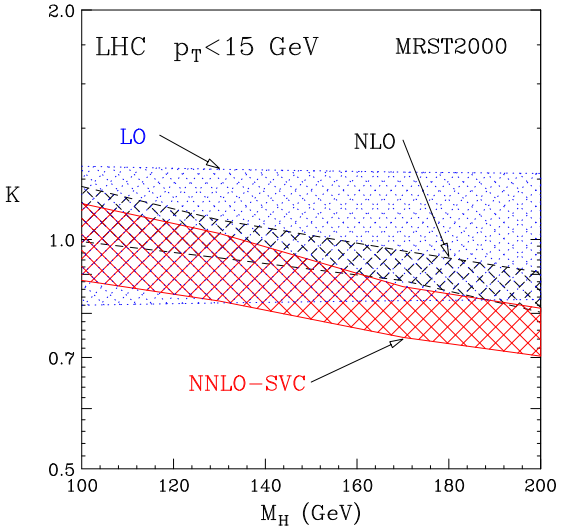

Figure 12: The same as in figure 8, but at the LHC and with $p_T^{cut} = 15\,\text{GeV}$.

conclusions about the inclusive production at the LHC were obtained in ref. [16]. The reliability of these NNLO approximations follows from the fact that a sizeable part of the higher-order QCD corrections to the partonic cross section is due to the emission of soft radiation, whereas the effect of hard radiation is suppressed by the steeply falling behaviour of the parton distributions at large x. As is customary practice, the perturbative expansion has been performed in the $\overline{\text{MS}}$ factorization scheme. Since the $\overline{\text{MS}}$-scheme parton densities embody (by definition) too much soft-gluon suppression (see e.g. ref. [40]), the perturbative corrections to the partonic cross section have to compensate for it; they thus enhance the hadronic cross section. At the Tevatron, we have shown that the NNLO effect is large and increases the cross section by about 50% with respect to the NLO result. This suggest that contributions beyond the NNLO can still be significant. Since Higgs boson production is less close to threshold at the LHC than at the Tevatron, the accompanying QCD radiation is less soft at the LHC than at the Tevatron. The estimated size of the NNLO effects at the LHC [16] is thus consistently smaller than at the Tevatron.

We have then addressed the impact of a jet veto on the inclusive cross section, both at the Tevatron and at the LHC. We have presented results at NLO and NNLO. At NNLO, we have used our estimate for the inclusive cross section and we have computed (subtracted) the effect of the jet veto by using the numerical program of ref. [27]. The jet veto reduces not only the absolute value of the cross section, but also the size of the higher-order QCD corrections. Since the accompanying QCD radiation is softer at the Tevatron than at the LHC, the impact of the veto is less effective at the Tevatron than at the LHC. In the case of a strong transverse-momentum cut of $p_T^{\text{veto}} = 15\,\text{GeV}$ at the Tevatron, the NNLO contributions increase the NLO result by about 25%. At the LHC, the difference between the NNLO and NLO results is already reduced to less than 10% by considering a weaker cut of $p_T^{\text{veto}} = 30\,\text{GeV}$. By further decreasing p_T^{veto}, perturbative contributions beyond the NNLO can become sizeable, since they are enhanced by powers of logarithmic terms of the type $\ln p_T^{\text{veto}}$.

JHEP01(2002)015

In this paper we have limited our analysis to the SM Higgs boson. The NLO QCD corrections to Higgs boson production within the Minimal Supersymmetric extension of the Standard Model (MSSM) are known [14, 41, 9]; for small values ($\tan\beta \lesssim 5$) of the MSSM parameter $\tan\beta$, they are comparable to those for the SM Higgs. This suggests that this similarity of the size of the perturbative QCD corrections remains true also at NNLO.

In actual experiments at hadron colliders, the observed cross section for Higgs signal events can significantly depend on the details of the experimental analysis. This is particularly true when a jet veto procedure is applied, because of effects due to efficiency for jet reconstruction, jet energy calibration, presence of pile-up events and so forth. Quantitative estimates of these effects require event simulations [6, 7] based on parton shower Monte Carlo generators [42, 43]. The parton shower produces multi-parton configurations that approximate the exact QCD matrix elements, but such approximation does not strictly correspond to the perturbative expansion of the cross section at LO, NLO, NNLO and so forth. Therefore, the NLO or NNLO K-factors computed in this paper cannot naively be used to rescale the results of present Monte Carlo simulations at the Tevatron and the LHC. As is customary practice in QCD analyses, more refined studies, which combine the perturbative QCD predictions with the Monte Carlo simulations at the detector level, are necessary to firmly quantify the expected number of veto selected Higgs events at the Tevatron and the LHC.

Acknowledgments

Part of this work was performed during the Workshop on 'Physics at TeV Colliders' (Les Houches, France, May 2001). We would like to thank Elzbieta Richter-Was for many useful discussions and comments. We also thank Thomas Gehrmann and Stefano Moretti for comments on the draft.

References

[1] For a review on Higgs physics in and beyond the Standard Model, see J.F. Gunion, H.E. Haber, G.L. Kane and S. Dawson, *The Higgs hunter's guide*, Addison-Wesley, Reading, Mass. 1990.

[2] LEP Higgs Working Group for Higgs boson searches collaboration, *Search for the standard model Higgs boson at LEP*, hep-ex/0107029.

[3] P. Igo-Kemenes, presentation given at the open session of the LEP Experiments Committee Meeting, 3 November 2000
(see: http://lepHiggs.web.cern.ch/LEPHIGGS/talks/index.html).

[4] ALEPH collaboration, R. Barate et al., *Observation of an excess in the search for the standard model Higgs boson at ALEPH*, *Phys. Lett.* **B 495** (2000) 1 [hep-ex/0011045];
L3 collaboration, M. Acciarri et al., *Higgs candidates in e^+e^- interactions at $\sqrt{s} = 206.6$ GeV*, *Phys. Lett.* **B 495** (2000) 18 [hep-ex/0011043];
DELPHI collaboration, P. Abreu et al., *Search for the standard model Higgs boson at LEP in the year 2000*, *Phys. Lett.* **B 499** (2001) 23 [hep-ex/0102036];

OPAL collaboration, G. Abbiendi et al., *Search for the standard model Higgs boson in e^+e^- collisions at $\sqrt{s} = 192\ GeV$–$209\ GeV$*, *Phys. Lett.* **B 499** (2001) 38 [hep-ex/0101014];
L3 collaboration, P. Achard et al., *Standard model Higgs boson with the l3 experiment at LEP*, *Phys. Lett.* **B 517** (2001) 319 [hep-ex/0107054].

[5] LEP collaborations, the LEP Electroweak Working Group and the SLD Heavy Flavour and Electroweak Working Group, CERN report LEPEWWG/2001-01.

[6] M. Carena et al., *Report of the tevatron Higgs working group*, hep-ph/0010338.

[7] CMS collaboration, *Technical proposal*, report CERN/LHCC/94-38 (1994);
ATLAS collaboration, *ATLAS detector and physics performance: technical design report*, volume 2, report CERN/LHCC/99-15 (1999).

[8] H.M. Georgi, S.L. Glashow, M.E. Machacek and D.V. Nanopoulos, *Higgs bosons from two gluon annihilation in proton-proton collisions*, *Phys. Rev. Lett.* **40** (1978) 692.

[9] M. Spira, *QCD effects in Higgs physics*, *Fortschr. Phys.* **46** (1998) 203 [hep-ph/9705337].

[10] C.A. Nelson, *Correlation between decay planes in Higgs boson decays into W pair (into Z pair)*, *Phys. Rev.* **D 37** (1988) 1220;
M. Dittmar and H. Dreiner, *How to find a Higgs boson with a mass between* $155\ GeV$ *to* $180\ GeV$ *at the LHC*, *Phys. Rev.* **D 55** (1997) 167 [hep-ph/9608317].

[11] T. Han and R.-J. Zhang, *Extending the Higgs boson reach at upgraded tevatron*, *Phys. Rev. Lett.* **82** (1999) 25 [hep-ph/9807424];
T. Han, A.S. Turcot and R.-J. Zhang, *Exploiting $h \to W^*W^*$ decays at the upgraded Fermilab Tevatron*, *Phys. Rev.* **D 59** (1999) 093001 [hep-ph/9812275].

[12] S. Dawson, *Radiative corrections to Higgs boson production*, *Nucl. Phys.* **B 359** (1991) 283.

[13] A. Djouadi, M. Spira and P.M. Zerwas, *Production of Higgs bosons in proton colliders: QCD corrections*, *Phys. Lett.* **B 264** (1991) 440.

[14] M. Spira, A. Djouadi, D. Graudenz and P.M. Zerwas, *Higgs boson production at the LHC*, *Nucl. Phys.* **B 453** (1995) 17 [hep-ph/9504378].

[15] M. Kramer, E. Laenen and M. Spira, *Soft gluon radiation in Higgs boson production at the LHC*, *Nucl. Phys.* **B 511** (1998) 523 [hep-ph/9611272].

[16] S. Catani, D. de Florian and M. Grazzini, *Higgs production in hadron collisions: soft and virtual QCD corrections at NNLO*, *J. High Energy Phys.* **05** (2001) 025 [hep-ph/0102227].

[17] R.V. Harlander and W.B. Kilgore, *Soft and virtual corrections to $pp \to H + X$ at NNLO*, *Phys. Rev.* **D 64** (2001) 013015 [hep-ph/0102241].

[18] R.V. Harlander, *Virtual corrections to $gg \to H$ to two loops in the heavy top limit*, *Phys. Lett.* **B 492** (2000) 74 [hep-ph/0007289].

[19] J.M. Campbell and E.W.N. Glover, *Double unresolved approximations to multiparton scattering amplitudes*, *Nucl. Phys.* **B 527** (1998) 264 [hep-ph/9710255].

[20] S. Catani and M. Grazzini, *Infrared factorization of tree level QCD amplitudes at the next-to-next-to-leading order and beyond*, *Nucl. Phys.* **B 570** (2000) 287 [hep-ph/9908523].

JHEP01(2002)015

[21] Z. Bern, V. Del Duca and C.R. Schmidt, *The infrared behavior of one-loop gluon amplitudes at next-to-next-to-leading order*, *Phys. Lett.* **B 445** (1998) 168 [hep-ph/9810409];
Z. Bern, V. Del Duca, W.B. Kilgore and C.R. Schmidt, *The infrared behavior of one-loop QCD amplitudes at next-to-next-to-leading order*, *Phys. Rev.* **D 60** (1999) 116001 [hep-ph/9903516].

[22] S. Catani and M. Grazzini, *The soft-gluon current at one-loop order*, *Nucl. Phys.* **B 591** (2000) 435 [hep-ph/0007142].

[23] T. Matsuura, S.C. van der Marck and W.L. van Neerven, *The calculation of the second order soft and virtual contributions to the Drell-Yan cross-section*, *Nucl. Phys.* **B 319** (1989) 570.

[24] A.D. Martin, R.G. Roberts, W.J. Stirling and R.S. Thorne, *Estimating the effect of nnlo contributions on global parton analyses*, *Eur. Phys. J.* **C 18** (2000) 117 [hep-ph/0007099].

[25] W.L. van Neerven and A. Vogt, *Improved approximations for the three-loop splitting functions in QCD*, *Phys. Lett.* **B 490** (2000) 111 [hep-ph/0007362];
W.L. van Neerven and A. Vogt, *NNLO evolution of deep-inelastic structure functions: the singlet case*, *Nucl. Phys.* **B 588** (2000) 345 [hep-ph/0006154].

[26] S. Catani, D. De Florian and M. Grazzini, *Higgs production at hadron colliders in (almost) nnlo QCD*, presented at the 36th Rencontres de Moriond on QCD and Hadronic Interactions, Les Arcs, France, 17-24 March 2001 and at the 9th International Workshop on Deep Inelastic Scattering (DIS 2001), Bologna, Italy, 27 April – 1 May 2001 hep-ph/0106049.

[27] D. de Florian, M. Grazzini and Z. Kunszt, *Higgs production with large transverse momentum in hadronic collisions at next-to-leading order*, *Phys. Rev. Lett.* **82** (1999) 5209 [hep-ph/9902483].

[28] J.R. Ellis, M.K. Gaillard and D.V. Nanopoulos, *A phenomenological profile of the Higgs boson*, *Nucl. Phys.* **B 106** (1976) 292;
M.A. Shifman, A.I. Vainshtein, M.B. Voloshin and V.I. Zakharov, *Low-energy theorems for Higgs boson couplings to photons*, *Sov. J. Nucl. Phys.* **30** (1979) 711.

[29] K.G. Chetyrkin, B.A. Kniehl and M. Steinhauser, *Hadronic Higgs decay to order α_s^4*, *Phys. Rev. Lett.* **79** (1997) 353 [hep-ph/9705240];
Decoupling relations to $O(\alpha_s^3)$ and their connection to low-energy theorems, *Nucl. Phys.* **B 510** (1998) 61 [hep-ph/9708255].

[30] A.P. Contogouris, N. Mebarki and S. Papadopoulos, *The dominant part of higher order corrections in perturbative QCD*, *Int. J. Mod. Phys.* **A 5** (1990) 1951.

[31] M. Gluck, E. Reya and A. Vogt, *Dynamical parton distributions revisited*, *Eur. Phys. J.* **C 5** (1998) 461 [hep-ph/9806404].

[32] CTEQ collaboration, H.L. Lai et al., *Global QCD analysis of parton structure of the nucleon: CTEQ5 parton distributions*, *Eur. Phys. J.* **C 12** (2000) 375 [hep-ph/9903282].

[33] J. Huston, S. Kuhlmann, H.L. Lai, F. Olness, J.F. Owens, D.E. Soper and W.K. Tung, *Study of the uncertainty of the gluon distribution*, *Phys. Rev.* **D 58** (1998) 114034 [hep-ph/9801444].

[34] R.V. Harlander and W.B. Kilgore, *Inclusive Higgs production at next-to-next-to-leading order*, hep-ph/0110200.

[35] C.R. Schmidt, *$H \to ggg(gq\bar{q})$ at two loops in the large-M_t limit*, *Phys. Lett.* **B 413** (1997) 391 [hep-ph/9707448].

JHEP01(2002)015

[36] S. Dawson and R.P. Kauffman, *Higgs boson plus multi-jet rates at the SSC*, *Phys. Rev. Lett.* **68** (1992) 2273;
R.P. Kauffman, S.V. Desai and D. Risal, *Production of a Higgs boson plus two jets in hadronic collisions*, *Phys. Rev.* **D 55** (1997) 4005 [hep-ph/9610541], erratum *ibid.* **58** (1997) 119901.

[37] R.K. Ellis, I. Hinchliffe, M. Soldate and J.J. van der Bij, *Higgs decay to $\tau^+\tau^-$: a possible signature of intermediate mass Higgs bosons at the SSC*, *Nucl. Phys.* **B 297** (1988) 221;
U. Baur and E.W.N. Glover, *Higgs boson production at large transverse momentum in hadronic collisions*, *Nucl. Phys.* **B 339** (1990) 38.

[38] V. Del Duca, W. Kilgore, C. Oleari, C. Schmidt and D. Zeppenfeld, *$H + 2$ jets via gluon fusion*, *Phys. Rev. Lett.* **87** (2001) 122001 [hep-ph/0105129];
V. Del Duca, W. Kilgore, C. Oleari, C. Schmidt and D. Zeppenfeld, *Gluon-fusion contributions to $H + 2$ jet production*, *Nucl. Phys.* **B 616** (2001) 367 [hep-ph/0108030].

[39] S. Frixione, Z. Kunszt and A. Signer, *Three-jet cross sections to next-to-leading order*, *Nucl. Phys.* **B 467** (1996) 399 [hep-ph/9512328];
S. Frixione, *A general approach to jet cross sections in QCD*, *Nucl. Phys.* **B 507** (1997) 295 [hep-ph/9706545].

[40] S. Catani, *Soft-gluon resummation: a short review*, in proc. of the 32nd Rencontres de Moriond *QCD and high-energy hadronic interactions*, J. Tran Than Van ed., Editions Frontières, Gif-sur-Yvette 1997, p. 331 [hep-ph/9709503].

[41] S. Dawson, A. Djouadi and M. Spira, *QCD corrections to SUSY Higgs production: the role of squark loops*, *Phys. Rev. Lett.* **77** (1996) 16 [hep-ph/9603423].

[42] G. Marchesini, B.R. Webber, G. Abbiendi, I.G. Knowles, M.H. Seymour and L. Stanco, *HERWIG: a Monte Carlo event generator for simulating hadron emission reactions with interfering gluons. Version 5.1 - april 1991*, *Comput. Phys. Commun.* **67** (1992) 465;
G. Corcella, I.G. Knowles, G. Marchesini, S. Moretti, K. Odagiri, P. Richardson, M.H. Seymour and B.R. Webber, *HERWIG 6: an event generator for hadron emission reactions with interfering gluons (including supersymmetric processes)*, *J. High Energy Phys.* **1** (2001) 010 [hep-ph/0011363].

[43] T. Sjostrand et al., *High-energy-physics event generation with PYTHIA 6.1*, *Comput. Phys. Commun.* **135** (2001) 238 [hep-ph/0010017].

JHEP01(2002)015